MATERIALS AND INTERFACES

Adsorptive Desulfurization with Xerogel-Derived Zinc-Based Nanocrystalline Aluminum Oxide

Xiangxin Yang,[†] Chundi Cao,[†] Kenneth J. Klabunde,[‡] Keith L. Hohn,[†] and Larry E. Erickson*,[†]

Department of Chemical Engineering, Kansas State University, Manhattan, Kansas 66506, and Department of Chemistry, Kansas State University, Manhattan, Kansas 66506

Adsorption of thiophene from a thiophene−pentane mixture has been investigated using zinc-based nanocrystalline aluminum oxide under ambient conditions. The adsorbents were prepared by a xerogel process, followed by thermovacuum treatment. The adsorptive experiments show that a 20 wt % Zn/Al_2O_3 adsorbent has the highest capacity, 2.8 mg/g (mg of sulfur per g of adsorbent). Brunauer−Emmett−Teller specific surface area (BET), X-ray diffraction (XRD), X-ray photoelectron spectroscopy (XPS), and transmission electron microscopy (TEM) were used to characterize the adsorbents. It was found that a spinel-phase $ZnAl_2O_4$ was formed during thermal treatment. The $ZnAl_2O_4$ spinel formed by thermal treatment in air was more crystalline, while thermal treatment under vacuum resulted in a defective, less crystalline spinel. Also, the particle size of the adsorbent was smaller and the surface area was higher when thermal treatment was under vacuum. In addition, the prepared adsorbents could be easily regenerated without losing capacity.

Introduction

Deep desulfurization of fuels has received more and more attention because sulfur oxide emissions generated by vehicle engines contribute to acid rain, poison catalysts in catalytic converters, and are an integral component in the cycle of atmospheric gas chemistry that leads to ozone production and smog.[1−4] As a result, the sulfur content in fuels has been gradually tightened. Interest in ultralow-sulfur fuels is also driven by fuel cells. However, catalysts used in the fuel processor are very sulfur sensitive. It is generally accepted that sulfur content in the fuels must be reduced to <1 ppmw for proton exchange membrane fuel cells.[5]

The state of the art in desulfurization technology is hydrodesulfurization (HDS), which has been used worldwide. In this process, under high temperature (300−340 °C) and high pressure (20−100 atm of H_2), sulfur-containing compounds are converted to H_2S and corresponding hydrocarbon on $CoMo/Al_2O_3$ or $NiMo/Al_2O_3$ catalysts.[6] The reactivity of organosulfur compounds varies widely depending on their structure and local sulfur atom environment.[7] Ultralow-sulfur specifications for fuels imply that more and more of the refractory sulfur-containing compounds need to be converted. This can only be achieved under severe reaction conditions with respect to pressure, temperature, and residence time, which significantly increases the cost of HDS. Consequently, development of new and affordable deep desulfurization processes for removing the refractory sulfur compounds is one of the major challenges for refineries and fuel-cell research.

Non-HDS-based desulfurization technologies have been reported in recent literature. Rhodococcus, considered to be the most promising biocatalyst, can selectively remove sulfur from sulfur-containing heterocyclic compounds.[8] Desulfurization via extraction using acetone, ethanol, polyethylene glycols, nitrogen-containing solvent, and ionic liquids indicates that such a process could be an alterative to HDS for deep desulfurization.[3,9,10] Oxidative desulfurization using hydrogen peroxide, molecular oxygen, or ultrasound has been reported.[11−13] Photooxidation desulfurization also shows a high selectivity to remove sulfur compounds.[14] Precipitation desulfurization has also been successfully applied in the removal of refractory dibenzothiophene derivatives.[15,16]

One of the new approaches for deep desulfurization is adsorption. Some organosulfur compounds are selectively adsorbed by solid adsorbents, while non-sulfur-containing compounds are left untouched at ambient temperature and pressure. A great deal of effort has been put into the search for new adsorbents and processes to remove sulfur from fuels, with goals of improvement of adsorption capacity, selectivity for organosulfur compounds, and regenerability, as well as elucidation of adsorptive mechanism.

Several Zn-based adsorbents, pure metal oxide (ZnO) and mixed-oxides (zinc ferrite and zinc titanate), have been attractive for gas-phase high-temperature desulfurization because of the favorable sulfidation thermodynamics, high H_2S removal efficiency, good sulfur-loading capacity, high regenerability, and sufficient strength.[17] Zinc was also the main component of a Ni/ZnO sorbent for adsorptive HDS of kerosene for fuel-cell applications, where ZnO in this system acts as an acceptor of sulfur that is released during regeneration of the sulfided nickel surface species.[18] In addition, Zn-zeolite X and Zn-zeolite Y have been used in the application of adsorptive desulfurization of transportation fuels.[19]

Nanocrystalline metal oxides constitute a novel family of inorganic porous materials, and they generally possess high surface areas.[20,21] The unique properties of nanocrystalline metal

* To whom correspondence should be addressed. Phone: 785-532-4313. Fax: 785-532-7372. E-mail: lerick@ksu.edu.

[†] Department of Chemical Engineering, Kansas State University.

[‡] Department of Chemistry, Kansas State University.

10.1021/ie0701928 CCC: $37.00
Published on Web 06/06/2007

oxides have been demonstrated for adsorptive desulfurization of model fuels.[22,23] The possible advantages of nanocrystalline metal oxide adsorbents compared with other conventional ones are as follows: high surface area, open pore structure with high pore volume, and the potential for preparing mixed nanocrystalline metal oxides with varying acidic/basic nature that will suit a particular application.[22] In this paper, we focus on the adsorption of thiophene using zinc-based nanocrystalline aluminum oxide at ambient conditions.

Experimental Section

Preparation of Adsorbents. The Zn/Al_2O_3 adsorbents were prepared by a xerogel process using zinc acetate and aluminum isopropoxide (98.0%, Aldrich). The general procedure consisted of the following steps. Aluminum isopropoxide (4.08 g, 0.02 mol) was dissolved in a mixture of 133 mL of toluene and 79 mL of ethanol. An appropriate amount of zinc acetate necessary to give the desired Zn loading was dissolved in 3 mL of deionized water. This zinc solution was added into the above mixture and the hydrolysis starts, followed by vigorous stirring at room temperature for 12 h. The final step was to dry the gel at around 70 °C, and the dry powder was ground and saved for later heating and use.

Characterization of Adsorbents. X-ray powder diffraction (XRD) patterns were obtained with a Bruker D8 diffractometer, using Cu Kα radiation (1.5406 Å) at 40 kV and 40 mA and a secondary graphite monochromator. Samples were packed into a plastic holder. The measurements were recorded in steps of 0.04° with a count time of 10 s in the 2θ range of 20−80°. Identification of the phases was made with the help of the Joint Committee on Powder Diffraction Standards (JCPDS) files.

X-ray photoelectron spectroscopy (XPS) data were recorded using a Perkin-Elmer PHI 5400 electron spectrometer. The spectrometer utilizes achromatized and monochromatized Al Kα radiation (1486.6 eV, 15 kV*300 W). The instrument operates at a pressure of about 2.0×10^{-9} Torr. The XPS binding energies were measured with a precision of 0.1 eV. Analyzer pass energy was set to 17.9 eV, and the contact time was 50 ms. Before the samples were tested, the spectrometer was calibrated by setting the binding energies of the Au $4f_{7/2}$ and Cu $2p_{3/2}$ to 84.0 and 932.7 eV, respectively. Binding energies for the samples were referenced to the C 1s line (284.6 eV).

N_2 adsorption−desorption isotherms were obtained at −196 °C using a computer-controlled NOVA 1000 instrument (Quantachrome, U.S.A.). Before adsorption, all the samples were degassed for 1 h at 150 °C under vacuum. The specific surface areas were estimated by the multipoint Brunauer−Emmett−Teller (BET) method. The Barett−Joyner−Halenda (BJH) method was applied to calculate the pore volume and the pore diameter.

Transmission electron microscopy (TEM) measurements were made with a JEOL 2000 EX electron microscope, equipped with a top entry stage. The powder was ultrasonically dispersed in acetone, and the suspension was deposited on a thin copper grid coated with a porous carbon film that supports the sample to be viewed. The grid was then placed in the electron beam between the filament and a phosphorus plate that lights up as electrons hit the surface. Electrons localized on atoms in the sample blocked the passage of the electron beam and appeared as dark areas on an otherwise illuminated image. The residual pressure at the specimen region was approximately 1×10^{-6} mbar.

Adsorption Experiments. Adsorption experiments were performed by a batch method. Adsorbent (0.3 g) was put in a heating tube and calcined under vacuum at 500 °C for 3 h; then the furnace was removed, and the heating tube was cooled down to room temperature; a model fuel (40 mL) consisting of pentane and thiophene (the sulfur level was 20 ppmw) was added, and the heating tube was sealed immediately. The mixture was kept at room temperature with vigorous stirring for a desired time, and the liquid phase was separated from the adsorbent. The final weight of different zinc loading adsorbents after the thermal vacuum treatment was in the range of 0.15−0.2 g because of the removal of organic impurities. The sulfur concentration in the solution was monitored by UV−vis spectrophotometry (thiophene has an absorption band at 231 nm, and the absorbance corresponds to the residual thiophene content). The experimental error was about ±2% based on our reproducible experiments. These experiments were not conducted in an inert gas or dry gas atmosphere.

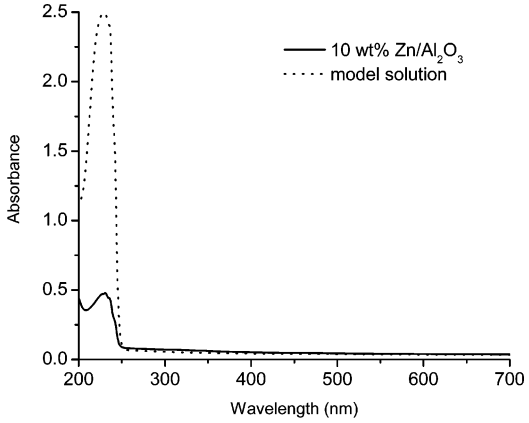

Figure 1. Adsorption of thiophene on 10 wt % Zn/Al_2O_3.

Table 1. Capacities for Adsorbents with Different Zinc Loadings[a]

	capacity ((mg of S)/(g of adsorbent))
5 wt % Zn/Al_2O_3	1.5
10 wt % Zn/Al_2O_3	2.0
15 wt % Zn/Al_2O_3	2.2
20 wt % Zn/Al_2O_3	2.8
25 wt % Zn/Al_2O_3	2.3

[a] Thermal treatment performed under vacuum for all samples.

Results and Discussion

Figure 1 showed the adsorption results on 10 wt % Zn/Al_2O_3 adsorbent. The intensity of absorbance at 231 nm decreased significantly after adsorption, suggesting that most of the thiophene was adsorbed out of the model fuel. It was clear that zinc-based alumina could be a good adsorbent for use in liquid-phase desulfurization at ambient conditions. The capacities of adsorbents with different zinc loadings, which were listed in Table 1, showed that 20 wt % Zn/Al_2O_3 had the highest capacity. For adsorbents having a zinc loading < 20 wt %, the capacity increased with higher zinc loadings. At a zinc loading > 20 wt %, the capacity decreased.

XRD. XRD can be used to identify crystalline bulk phases and the crystallinity, as well as to estimate particle size.[24] It was reported that, when transition metal ions were supported on alumina, two reactions occurred concurrently: one led to the formation of a spinel and the other led to a segregation of an oxide.[25] It was easy to identify the segregated oxide phase by the analysis of XRD data. The identification of the spinel phases was rather difficult because alumina had a defect spinel structure and its lattice parameters were almost identical to those of the spinel. It was found that the intensities of lines at $d =$

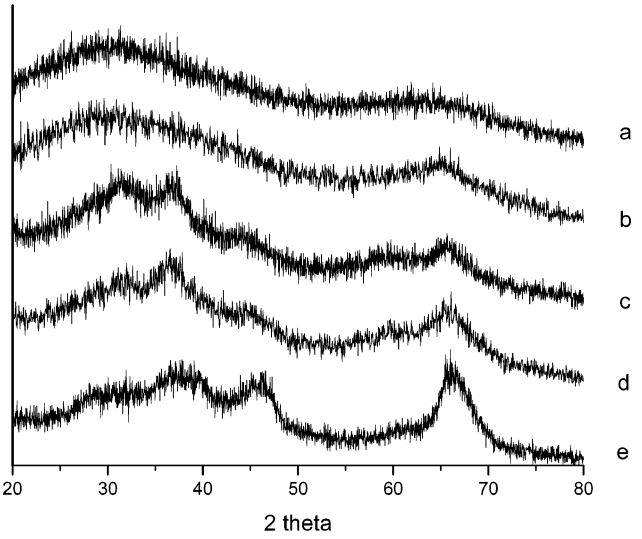

Figure 2. X-ray powder diffraction patterns of different zinc loading samples: (a) 20 wt % Zn/Al_2O_3; (b) 10 wt % Zn/Al_2O_3; (c) 20 wt % Zn/Al_2O_3; (d) 10 wt % Zn/Al_2O_3; and (e) Al_2O_3 (support) (a and b are samples calcined under vacuum at 500 °C for 3 h; c, d, and e are samples calcined in air at 500 °C for 3 h).

2.4 and 2.8 Å (strong lines for spinel, $2\theta = 32, 37°$) increased in the zinc metal ion containing alumina as compared with the pure alumina. So relative intensities of these two diffraction lines were used to identify the formation of the spinel-like structure.[25]

The experimental XRD patterns obtained for different zinc loadings were shown in Figure 2. All samples gave broad diffraction lines, suggesting low crystallinity. The intensities of the diffraction lines at about 31.4 and 36.8° for zinc-containing samples began to increase relative to the main alumina line ($2\theta = 46.0, 66.8°$). With increased zinc loading, the two lines became narrower and more intense, consistent with formation of a spinel-like phase. Although ZnO had diffraction lines at around 32 and 37°, other major lines in ZnO patterns (34.4 and 47.5°) were absent even for higher zinc loading sample (25 wt %, not shown here). However, we could not rule out the possible formation of ZnO (the crystallite size of ZnO was small and undetectable as a consequence of sensitivity and size limits of the XRD technique). It was obvious that, when calcined in air, the zinc ions interacted strongly with the Al_2O_3 support and formed a "surface spinel" that was similar in structure to bulk $ZnAl_2O_4$. In contrast, only two broad peaks appeared in the pattern when samples were treated under vacuum. The intensity of the broad peak in the 25−40° range increased with higher zinc loading relative to the peak in 60−75°. We believed that a surface spinel was also formed during vacuum treatment, but a more defective structure with more exposed zinc ions was formed, which resulted in broader peaks in the XRD pattern. The XPS and BET data discussed next showed further evidence of the formation of surface spinel and its smaller size.

XPS. XPS binding energies provide a means to identify the chemical composition of a sample as well as the difference in the oxidation state and molecular environment of identified elements. The Zn $2p_{1/2}$ and Zn $2p_{3/2}$ lines for 20 wt % Zn/Al_2O_3 with different treatments and reference compounds, Zn and ZnO, were shown in Figure 3.

The XPS binding energies for Zn $2p_{1/2}$ and Zn $2p_{3/2}$ were 1045.3 and 1022.2 eV, respectively, for the vacuum treatment sample; the respective values were 1045.5 and 1022.3 eV for the air treatment sample. As can be seen, calcination in air or under vacuum resulted in little chemical shift for Zn $2p_{1/2}$ and

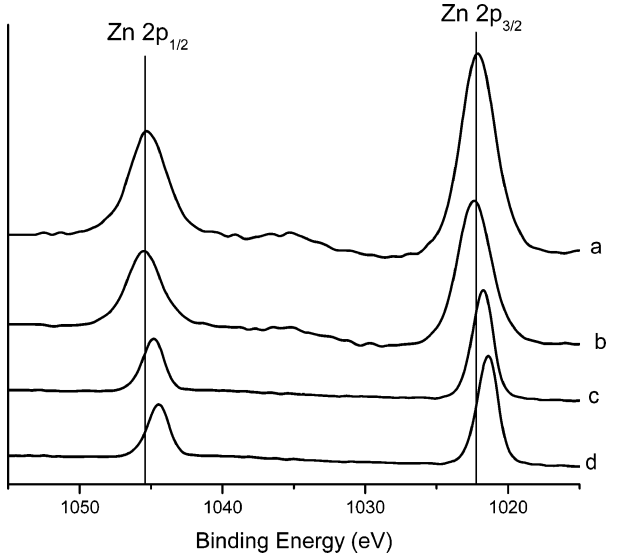

Figure 3. XPS spectra of Zn $2p_{3/2}$ and Zn $2p_{1/2}$ for different samples: (a) 20 wt % Zn/Al_2O_3 (500 °C, vacuum); (b) 20 wt % Zn/Al_2O_3 (500 °C, air); (c) ZnO; and (d) Zn.

Table 2. Pore Structure of Zn/Al_2O_3 Adsorbents

	surface area (m^2/g)	pore volume (cm^3/g)	pore diameter (nm)
5 wt % Zn/Al_2O_3 [a]	437	2.0	9
10 wt % Zn/Al_2O_3 [a]	377	1.4	4
20 wt % Zn/Al_2O_3 [a]	336	0.9	4
25 wt % Zn/Al_2O_3 [a]	278	0.8	4
20 wt % Zn/Al_2O_3 [b]	400	1.0	3

[a] Thermal treatment in air. [b] Thermal treatment under vacuum.

Zn $2p_{3/2}$ lines, indicating no change in the oxidation state of zinc for these two different thermal treatments. This also suggested that Zn^{2+} was not easily reduced, though autoreduction of many supported transition metals could occur under vacuum treatment.[1,23,26,27] The binding energies for Zn $2p_{3/2}$ on the two 20 wt % Zn/Al_2O_3 samples were 0.7 and 0.8 eV higher than that of ZnO and 0.9 and 1.0 eV higher than that of metallic Zn. The binding energies for both Zn $2p_{3/2}$ and Zn $2p_{1/2}$ lines were virtually identical with the values for $ZnAl_2O_4$ (1022.0 and 1045.1 eV)[28] and in good agreement with the formation of a surface spinel (bulklike $ZnAl_2O_4$) as indicated by XRD.

BET. The results in Table 2 showed the textural properties of adsorbents. The specific surface area decreased with an overall zinc content increase. The results showed that vacuum treatment greatly affected the textural properties of the adsorbent. For an adsorbent with 20 wt % zinc loading, the surface area was about 20% higher when thermal treatment was conducted under vacuum compared with that in air. In addition, the pore volume was almost the same and the pore diameter was smaller, suggesting a smaller particle size. This was also consistent with XRD indications.

TEM. TEM is one of the primary tools of materials chemists and is essential to accurately describe the size and shape of the particles. Electron micrographs of 20 wt % Zn/Al_2O_3 (calcined in air or under vacuum) were shown in Figure 4. It could be seen that the prepared samples had agglomerated to form larger particles. It could also be clearly seen that zinc was well-dispersed on the surface of the support and the samples consisted of agglomerates of primary particles with an average diameter of ca. 10 nm. There was no visible difference between these two samples with different thermal treatments. A deeper

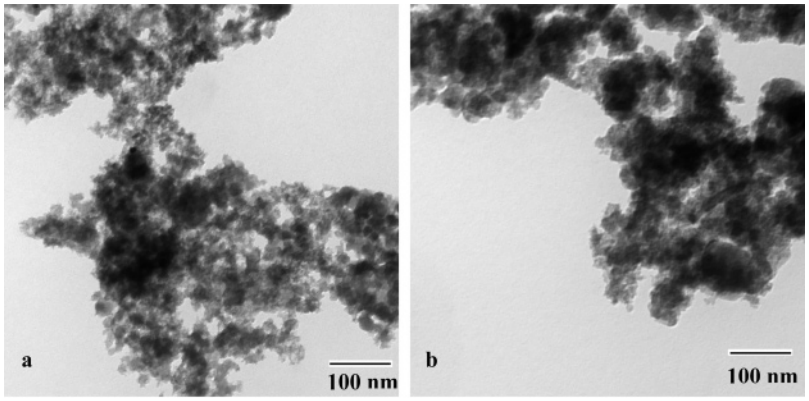

Figure 4. Electron micrographs of 20 wt % Zn/Al_2O_3 adsorbent (a) calcined in air and (b) calcined under vacuum.

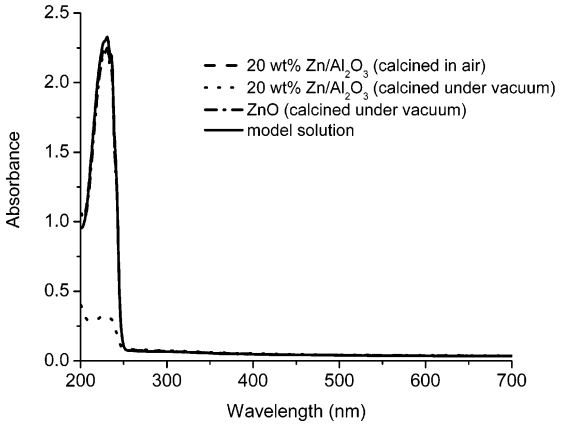

Figure 5. Adsorption of thiophene on ZnO and 20 wt % Zn/Al_2O_3 with different treatments.

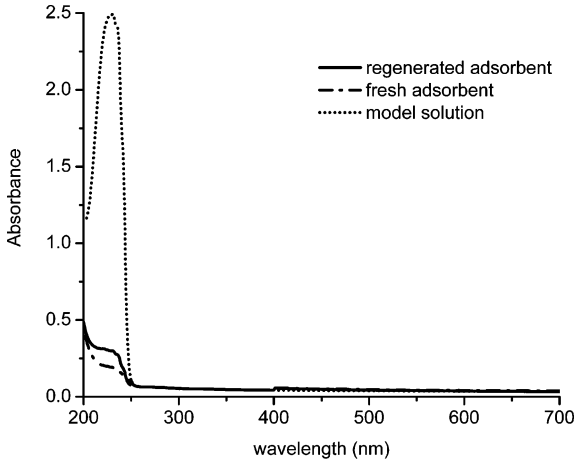

Figure 6. Adsorption of thiophene on fresh or regenerated 20 wt % Zn/Al_2O_3 adsorbent.

understanding of the difference in the surface structure and the particle size might be obtained with the help of a high-resolution TEM.

Importance of Vacuum Treatment. Figure 5 showed the performance of ZnO and 20 wt % Zn/Al_2O_3 adsorbent with different treatments. It was obvious that pure ZnO did not adsorb thiophene, and vacuum treatment was crucial for the adsorption of thiophene on the zinc-based adsorbents. In order to explain these particularly interesting results for zinc-based adsorbents treated under vacuum, we proposed that a less-ordered surface $ZnO-Al_2O_3$ structure was responsible for the adsorption of thiophene from the model fuel. When the thermal treatment was conducted in air, a more-ordered (crystalline) structure, probably with fewer surface exposed zinc ions, forms. On the other hand, zinc ions mixed less strongly with alumina because of the absence of oxygen when treatment was carried out under vacuum, which resulted in the stronger interaction between zinc ions and thiophene molecules during adsorption. In addition, when zinc loading increased from 20 to 25 wt %, the capacity decreased because of the formation of new zinc species, such as ZnO. Zinc ions preferably diffused into the vacant tetrahedral sites of the alumina lattice. If all of the available lattice sites were saturated, further addition of zinc could be accommodated only by segregation of a separate ZnO phase,[28] which was not very effective for thiophene adsorption.

Adsorbent Regeneration. The 20 wt % Zn/Al_2O_3 adsorbent was tested for regeneration after one adsorption cycle. The regeneration was achieved by heating the spent adsorbent at 500 °C for 1 h under vacuum to remove the adsorbed thiophene molecules. After the regeneration was completed, the adsorbent was mixed with fresh model solution at room temperature and the second adsorption cycle was performed. Figure 6 showed that >96% desulfurization capacity was recovered with the regeneration scheme. Thus, the adsorbent could be easily regenerated without losing capacity.

Conclusions

Xerogel-prepared zinc-based nanocrystalline alumina adsorbents have been demonstrated to be effective in the liquid-phase desulfurization at room temperature and pressure based on the batch method. Surface spinel was formed during thermal treatment because of the interaction between zinc ions and alumina. Compared with thermal treatment conducted in air, thermal vacuum treatment created a more defective structure with weaker interaction between zinc ions and alumina support, which resulted in the possibility of stronger interaction between zinc ions and thiophene molecules in the adsorption process and the removal of thiophene from the hydrocarbon solution. The experimental results showed the excellent regenerative property of the adsorbent by a simple regeneration scheme.

Acknowledgment

This work is partially supported through Kansas State University Targeted Excellence Program and NanoScale Corporation.

Literature Cited

(1) Hernandez-Maldonado, A. J.; Yang, R. T. Desulfurization of Transportation Fuels by Adsorption. *Catal. Rev.* **2004**, *46*, 111.

(2) Song, C. S. An Overview of New approaches to Deep Desulfurization for Ultra-Clean Gasoline, Diesel Fuel and Jet Fuel. *Catal. Today* **2003**, *86*, 211.

(3) Babich, I. V.; Moulijn, J. A. Science and Technology of Novel Processes for Deep Desulfurization of Oil Refinery Streams: A Review. *Fuel* **2003**, *82*, 607.

(4) Whitehurst, D. D.; Isoda, T.; Mochida, I. Present State of the Art and Future Challenges in the Hydrosulfurization of Polyaromatic Sulfur Compounds. *Adv. Catal.* **1998**, *42*, 345.

(5) Kim, J. H.; Ma, X. L.; Zhou, A.; Song, C. S. Ultra-deep Desulfurization and Denitrogenation of Diesel Fuel by Selective Adsorption Over Three Different Adsorbents: A Study on Adsorptive Selectivity and Mechanism. *Catal. Today* **2006**, *111*, 74.

(6) Gates, B. C.; Katzer, J. R.; Schuit, G. C. *Chemistry of Catalysis Processes*; McGraw-Hill: New York, 1979.

(7) Mochida, I.; Choi, K. H. An Overview of Hydrodesulfurization and Hydrodenitrogenation. *J. Jpn. Pet. Inst.* **2004**, *47* (3), 145.

(8) Mcfarland, B. L.; Boron, D. J.; Deever, W.; Meyer, J. A.; Johnson, A. R.; Atlas, R. M. Biocatalytic Sulfur Removal from Fuels: Applicability for producing Low Sulfur Gasoline. *Crit. Rev. Microbiol.* **1998**, *24* (2), 99.

(9) Eber, J.; Wasserscheid, P.; Jess, A. Deep Desulfurization of Oil Refinery Streams by Extration with Ionic Liquids. *Green Chem.* **2004**, *6*, 316.

(10) Zhang, S. G.; Zhang, Z. C. Novel Properties of Ionic Liquids in Selective Sulfur Removal from Fuels at Room Temperature. *Green Chem.* **2002**, *4*, 376.

(11) Filippis, P. D.; Scarsella, M. Oxidative Desulfurization: Oxidation Reactivity of Sulfur Compounds in Different Organic Matrixes. *Energy Fuels* **2003**, *17*, 1452.

(12) Murata, S.; Murata, K.; Kidena, K.; Nomura, M. A Novel Oxidative Desulfurization System for Diesel Fuels with Molecular Oxygen in the Presence of Coblat Catalysts and Aldehydes. *Energy Fuels* **2004**, *18*, 116.

(13) Mei, H.; Mei, B. W.; Yen, T. F. A New Method for Obtaining Ultra-low Sulfur Diesel Fuel via Ultrasound Assisted Oxidative Desulfurization. *Fuel* **2003**, *82* (4) , 405

(14) Shiraishi, Y.; Hirai, T.; Komasawa, I. Photochemical Desulfurization and Denitrogenation Process forVacuum Gas Oil Using an Organic Two-Phase Extraction System. *Ind. Eng. Chem. Res.* **2001**, *40*, 293.

(15) Sevignon, M.; Macaud, M.; Favre-Reguillon, A.; Schulz, J.; Rocault, M.; Faure, R.; Vrinat, M.; Lemaire, M. Ultra-deep Desulfurization of Transportation Fuel via Charge-Transfer Complexes under Ambient Conditions. *Green Chem.* **2005**, *7*, 413.

(16) Milenkovic, A.; Schulz, E.; Meille, V.; Loffreda, D.; Forissier, M.; Vrinat, M.; Sautet, P.; Lemaire, M. Selective Elimination of Alkyldibenzothiophenes from Gas Oil by Formation of Insoluble Charge-Transfer-Complexes. *Energy Fuels* **1999**, *13*, 881.

(17) Li, Z. J.; Flytzani-Stephanopoulos, M. Cu−Cr−O and Cu−Ce−O Regenerable Oxide Sorbents for Hot Gas Desulfurization. *Ind. Eng. Chem. Res.* **1997**, *36*, 187.

(18) Tawara, T.; Nishimura, T.; Iwanami, H.; Nishimoto, T.; Hasuike, T. New Hydrodesulfurization Catalyst for Petroleum-fed Fuel Cell Vehicles and Cogenerations. *Ind. Eng. Chem. Res.* **2001**, *40*, 2367.

(19) Hernandez-Maldonado, A. J.; Yang, F. H.; Qi, G. S.; Yang, R. T. Desulfurization of Transportation Fuels by π-complexation Sorbents: Cu-(I)-, Ni(II)-, and Zn(II)-zeolites. *Appl. Catal., B* **2005**, *56*, 111.

(20) Klabunde, K. J.; Stark, J.; Koper, O.; Mohs, C.; Park, D. G.; Decker, S.; Jiang, Y.; Lagadic, I.; Zhang, D. Nanocrystals as Stoichiometric Reagents with Unique Surface Chemistry. *J. Phys. Chem.* **1996**, *100*, 12142.

(21) Richards, R.; Li, W.; Decker, S.; Davidson, C.; Koper, O.; Volodin, A.; Rieker, T.; Klabunde, K. J. Consolidation of Metal Oxide Nanocrystals. Reactive Pellets with Controllable Pore Structure That Represent a New Family of Porous, Inorganic Materials. *J. Am. Chem. Soc.* **2000**, *122*, 4921.

(22) Jeevanandam, P.; Klabunde, K. J.; Tetzler, S. H. Adsorption of Thiophenes out of Hydrocarbons Using Metal Impregnated Nanocrystalline Aluminum Oxide. *Microporous Mesoporous Mater.* **2005**, *79*, 101.

(23) Yang, X.; Erickson, L. E.; Hohn, K. L.; Jeevanandam, P.; Klabunde, K. J. Sol-Gel Cu−Al_2O_3 Adsorbents for Selective Adsorption of Thiophene out of Hydrocarbon. *Ind. Eng. Chem. Res.* **2006**, *45*, 6169.

(24) Warren, B. E. *X-ray Diffraction*; Addison-Wesley: Reading, MA, 1969.

(25) Lo Jacono, M.; Schiavello, M. *Preparation of Catalysts*; Elsevier: Amsterdam, The Netherlands, 1976.

(26) Hernandez-Maldonado, A. J.; Yang, R. T. Desulfurization of Liquid Fuels by Adsorption via π Complexation with Cu(I)−Y and Ag−Y Zeolites. *Ind. Eng. Chem. Res.* **2003**, *42*, 123.

(27) Yang, R. T. *Adsorbents: Fundamentals and Applications*; Wiley: New York, 2003.

(28) Strohmeier, B. R.; Hercules, D. M. Surface Spectroscopic Characterization of the Interaction between Zinc Ions and γ-Alumina. *J. Catal.* **1984**, *86*, 266.

Received for review February 2, 2007
Revised manuscript received April 23, 2007
Accepted April 30, 2007

IE0701928